

Article

Seasonal Phytoplankton Characteristics Related with Region-Specific Coastal Environments in the Korean Peninsula

Chung Hyeon Lee ¹, Young Kyun Lim ¹, Mungi Kim ², Seongjin Hong ^{2,3} and Seung Ho Baek ^{1,*}

¹ Ecological Risk Research Department, KIOST (Korea Institute of Ocean Science and Technology), Geoje 53201, Republic of Korea

² Department of Earth, Environmental & Space Sciences, Chungnam National University, Daejeon 34134, Republic of Korea; hongseongjin@gmail.com (S.H.)

³ Department of Marine Environmental Sciences, Chungnam National University, Daejeon 34134, Republic of Korea

* Correspondence: baeksh@kiost.ac.kr

Abstract: The seasonal dynamics of phytoplankton communities in Korean coastal waters (KCWs) are influenced by complex interactions between ocean currents and nearshore human activities. Despite these influences, the understanding of seasonal phytoplankton changes and their environmental relationships in KCWs remains limited. We investigate the influence of the distinct characteristics of the three seas surrounding the KCWs (the Yellow Sea, the South Sea, and the East Sea) on seasonal phytoplankton communities based on field surveys conducted at 23 stations between 2020 and 2021. The East Sea exhibited higher winter temperatures due to the Jeju and Tsushima warm currents, while summer temperatures were lower compared to the other regions, highlighting the role of currents and deeper oceanic waters. The Yellow Sea showed significant freshwater influence with low salinity levels from major rivers, contrasting with the higher salinity in the East Sea. These differences led to a disparity in the productivity of the two regions: the highest value of Chl. *a* was observed to be 6.05 $\mu\text{g L}^{-1}$ in the Yellow Sea in summer. Diatoms dominated in nutrient-rich conditions, particularly in the Yellow Sea, where they comprised up to 80–100% of the phytoplankton community in summer, winter, and spring. PCA analysis revealed positive correlations between diatoms and Chl. *a*, while cryptophytes, which thrive in the absence of diatom proliferation, showed no such correlation, indicating their opportunistic growth in nutrient-limited conditions. This study highlights the significant impact of region-specific hydrographic factors on phytoplankton communities in KCWs, with diatoms dominating in summer and cryptophytes and dinoflagellates showing seasonal and regional variations. Understanding these dynamics is crucial for predicting phytoplankton bloom dynamics and their ecological implications in coastal ecosystems.

Keywords: Korean coastal waters; regional differences; seasonality; phytoplankton community; ocean current

Citation: Lee, C.H.; Lim, Y.K.; Kim, M.; Hong, S.; Baek, S.H. Seasonal Phytoplankton Characteristics Related with Region-Specific Coastal Environments in the Korean Peninsula. *J. Mar. Sci. Eng.* **2024**, *12*, 1008. <https://doi.org/10.3390/jmse12061008>

Academic Editors: Terry E. Whitedge

Received: 29 May 2024

Revised: 10 June 2024

Accepted: 13 June 2024

Published: 17 June 2024



Copyright: © 2024 by the authors. Licensee MDPI, Basel, Switzerland. This article is an open access article distributed under the terms and conditions of the Creative Commons Attribution (CC BY) license (<https://creativecommons.org/licenses/by/4.0/>).

1. Introduction

Phytoplankton comprise a highly diverse group of microorganisms, distributed in nutrient-rich areas of the world's oceans, and contribute to more than 50% of the global net primary production, particularly notable in coastal regions [1]. Primarily autotrophic, phytoplankton provide various ecosystem services such as oxygen release and carbon dioxide sequestration [2]. Through the process of photosynthesis, they form the foundation of marine food webs, supporting the production of numerous species, including those at higher trophic levels with significant commercial value. In coastal waters, ecologically and economically valuable marine species (e.g., fish, crabs, shrimp) are closely linked to the productivity and biomass of phytoplankton, the base of the food web [3]. In particular, coastal zones are highly sensitive and vulnerable to environmental change due to high

human population density and complex interactions between land and ocean [4,5]. Temperate coastal waters are recognized as global hotspots of marine diversity. Conversely, poor seawater circulation in inland bays and estuaries can result in nutrient overloading, leading to negative impacts on ecosystems through extensive phytoplankton blooms [6].

Phytoplankton can respond quickly to environmental change, and their seasonal cycles and succession are influenced by both bottom-up factors, such as water temperature and nutrient availability, and top-down factors, such as zooplankton feeding interactions [7–9]. In particular, change of water temperature and anthropogenic nutrient load are important environmental factors in determining seasonal changes in phytoplankton composition. In addition, seasonal patterns in phytoplankton can be partially understood by considering functional differences between phytoplankton groups [10,11], which are associated with species-specific ecological and physiological characteristics [12,13]. Therefore, species-specific characteristics of phytoplankton based on functional groups may provide important clues for effective resource utilization during seasonal succession and competitive relationships among dominant phytoplankton [11,14].

The Korean Peninsula is bordered by the Yellow Sea to the west, the South Sea (connecting to the East China Sea) to the south, and the East Sea (Sea of Japan) to the east (Figure 1). The Yellow Sea is a shallow, semi-enclosed area with a depth of about 50–100 m, bordering Korea and China [15]. The coastal region in the Yellow Sea is known for its low water depth, large tidal range, and rapid ocean circulation, making it an important area for marine fisheries production related with high primary productivity [16,17]. The coastal waters of the South Sea, with a depth of about 100 m, are strongly influenced by the Kuroshio warm current, especially the Jeju warm current (JWC) and the Tsushima warm current (TWC), which are tributaries of the Kuroshio Current and are characterized by high salinity and water temperature [15]. Especially during the autumn and winter months, the TWC strongly influences the water-quality characteristics of the South Sea and East Sea regions of Korea. The East Sea is a large body of water with an average depth of 1800 m located between the Eurasian continent and Japan. The East Sea interacts with the TWC of the Kuroshio turbulence and the North Korean cold current (NKCC) of the cold Riemannian turbulence. These dynamics lead to the formation of a distinct subpolar front near 38–40 °N, where the warm-water mass of the East Korean warm current (EKWC) meets the cold-water mass of the North Korean cold current (NKCC) [18–21].

The winter monsoon season, in particular, exerts a significant influence on coastal waters by reducing water temperatures and intensifying water mixing [22]. Although nutrient inputs from land are typically reduced during the winter due to lower rainfall, water mixing in winter promotes nutrient transport from the bottom to the surface euphotic layer, resulting in high nutrients in the whole water column [23,24]. Conversely, summers are characterized by hot and humid conditions, with freshwater runoff carrying land-derived nutrients into coastal waters due to heavy rainfall, leading to low salinity. During spring and autumn, consistent water column mixing maintains moderate nutrient levels, triggering substantial phytoplankton blooms. These changes in environmental factors are expected to result in changes in the composition of phytoplankton communities, especially in warmer waters. In particular, our previous study demonstrated the characteristics of environmental factors related with winter phytoplankton and bacterial population dynamics [25]. However, there remains a knowledge gap regarding the interactions between phytoplankton community structure characteristics and geographically based environmental factors across the coastal waters of the Korean Peninsula throughout four seasons. This study aims to establish baseline data to assess how region-specific environmental factors influence phytoplankton communities in coastal waters across three geographical regions of the Korean Peninsula, seasonally.

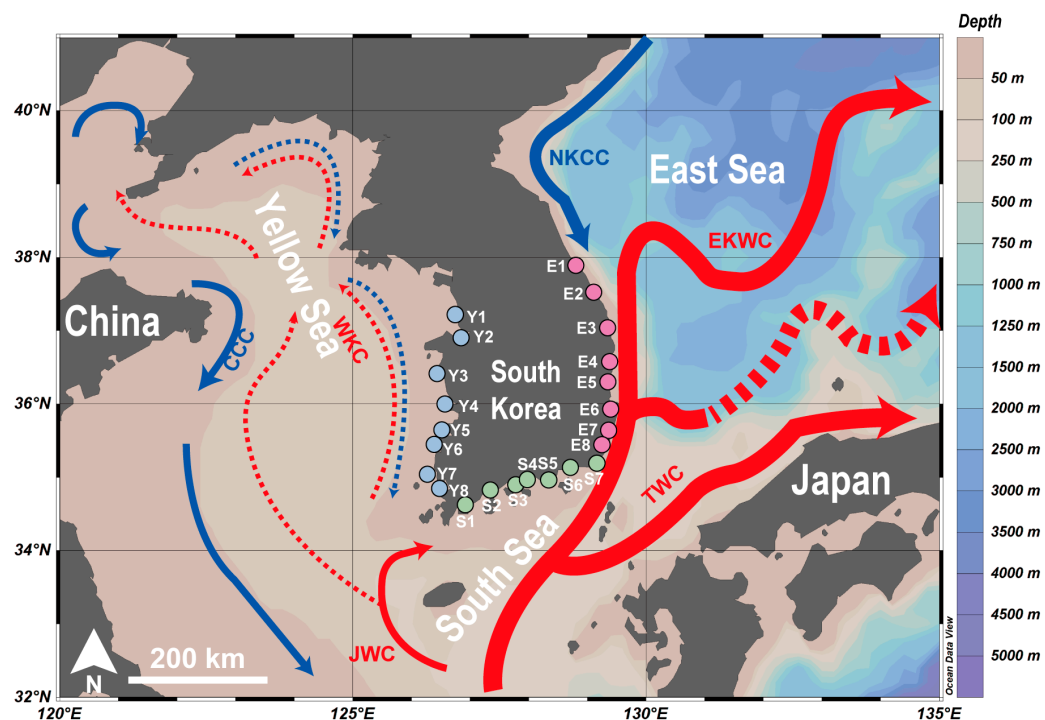


Figure 1. Sampling stations (circles) and ocean currents (red arrows: warm currents, blue arrows: cold currents), including Tsushima warm current (TWC), Jeju warm current (JWC), East Korean warm current (EKWC), West Korean current (WKC), China cold current (CCC), North Korean cold current (NKCC).

2. Materials and Methods

2.1. Field Sampling

Field sampling was conducted at eight stations (Y1–Y8) in the Yellow Sea, eight stations (S1–S8) in the South Sea, and seven stations (E1–E7) in the East Sea along the Korean coastal waters (KCWs) in August 2020, November 2020, February 2021, and April 2021 (Figure 1; the depths at the survey stations were less than 50 m). In situ measurements of water quality parameters, including temperature, salinity, pH, and dissolved oxygen (DO), were performed at the surface using YSI EXO2 Sonde probes (Yellow Springs, OH, USA). Surface water samples were collected with a bucket at all stations. For chlorophyll *a* (Chl. *a*) measurements, 100–300 mL (depended on seasonality) of water was collected, immediately filtered through a 47 mm diameter GF/F filter with a pore size of 0.45 μm (Whatman), and processed on site. The filtrates were transferred to acid-cleaned 15-mL conical tubes (SPL Life Sciences, Pocheon, Republic of Korea), and HgCl_2 was added to a final concentration of 0.1% to inhibit biological activity. Both filters and filtrates were stored in a dry ice box at $-20\text{ }^\circ\text{C}$ in the dark until laboratory analysis. Phytoplankton samples, consisting of 500 mL of surface water, were preserved immediately in polyethylene bottles with Lugol’s solution at a final concentration of 3% and stored at room temperature in the dark until analysis. Focusing on identifying seasonality, we conducted an analysis that included the winter data from February 2021 used by Lim et al. [25].

2.2. Sample Analyses

For laboratory analysis of field samples, chlorophyll *a* (Chl. *a*) was measured in the laboratory using a fluorometer (Turner BioSystems, Sunnyvale, CA, USA) calibrated with a Chl. *a* standard (SKU: 10-850; Turner Design, San Jose, CA, USA) and installed with an optical filter (10-037R; Turner Design, San Jose, CA, USA) for measuring extractive and in vivo chlorophyll (Turner Design, San Jose, CA, USA). The fluorometer was periodically validated for Chl. *a* with a solid secondary standard (10-AU-904; Turner Design, San Jose,

CA, USA). The extraction of filtered material was performed with 90% acetone at room temperature for 24 h in darkness. The concentrations of inorganic nutrients (ammonia, nitrate, nitrite, phosphate, and silicate) were measured using a flow injection autoanalyzer (QuikChem 8000; Lachat Instruments, Loveland, CO, USA), which was calibrated using Reference Materials for Nutrients in Seawater (RMNS, KANSO Technos Co., Ltd., Osaka, Japan). For counting and identifying phytoplankton, each 0.5 L Lugol's fixed sample was concentrated to approximately 50 mL by decanting the supernatant, as described in Sournia [26]. The concentrated subsamples were loaded onto a Sedgewick–Rafter counting chamber after gentle mixing, and phytoplankton were counted using a light microscope (Carl Zeiss; Gottingen, Germany) at 200× magnification. The identification of phytoplankton was performed based on their morphological features under a light microscope at 400× magnification, referring to phytoplankton identification guides by Omura et al. [27].

2.3. Remote Sensing Analyses

Satellite-derived data on surface temperature, salinity, and chlorophyll *a* concentrations were provided by the Japan Aerospace Exploration Agency (JAXA) in this study. These images were based on the JAXA remote sensing reflectance data and taken in summer on 14 August and in autumn on 17 November, both seasons observed in 2020, and in winter on 2 February and in spring on 19 April, both seasons observed in 2021. These dates were chosen based on field sampling dates.

2.4. Statistical Analysis

Variations in phytoplankton abundance, environmental factors, and nutrient concentrations across KCWs including the Yellow Sea, South Sea, and East Sea did not consistently meet the assumptions of normality and equality of variances required for one-way analysis of variance (ANOVA). Consequently, the non-parametric Kruskal–Wallis test was applied, followed by the Mann–Whitney U-test for post hoc pairwise comparisons, with a Bonferroni correction set at $p = 0.017$ (equivalent to $p < 0.05/3$), using SPSS version 25 (Chicago, IL, USA). Principal component analysis (PCA) was utilized to explore the associations among predominant phytoplankton (maximum composition >50%), environmental factors (temperature, dissolved oxygen, salinity, pH, and chlorophyll *a*), and nutrient concentrations (nitrite+nitrate, ammonium, phosphate, and silicate), and to identify the variables exerting the most significant influences at different stations in Korean coastal waters, this was performed in R version 4.2.1. Additionally, in the PCA analysis, the boundary represents the 95% confidence interval, which was obtained using the R package 'ellipse'.

3. Results

3.1. Environmental Factors in Three Geographical Regions

The highest water temperatures were recorded during summer, while the lowest occurred in winter. Seasonal averaged temperatures changed to 25.7 ± 2.6 °C in summer, 16.2 ± 1.0 °C in autumn, 7.2 ± 3.2 °C in winter, and 13.7 ± 2.0 °C in spring (Figure 2a). Although there was a significant difference between spring and summer seasons ($p < 0.001$), similar trends were observed between spring and autumn. Notably, in autumn 2020, water temperatures in the East Sea, which influence the warm current, were higher than to the other two regions. On the other hand, in spring and summer, the temperatures in the East Sea were relatively lower than those in the Yellow Sea and South Sea. Conversely, in winter, water temperatures in the Yellow Sea (Sites Y1–Y7) at shallow depths significantly dropped to 4 °C, consistently lower than those at the South Sea and East Sea sites of the Korean Peninsula (Kruskal–Wallis test; $p < 0.05$). The average salinity in each geographical region ranged from 26.5 in the Yellow Sea in summer to >34 during winter and spring. Seasonally, surface salinity was relatively low in summer and high in winter, autumn, and spring. Overall, salinity levels in the Yellow Sea were generally lower than

those in the South Sea and East Sea (Figure 2b). On the other hand, pH levels were lower in autumn and spring and higher in summer and winter (Figure 2c). Overall, pH levels in the East Sea were higher than those in the South Sea and Yellow Sea during all seasons. Dissolved oxygen (DO) levels were lower in summer and autumn and higher in winter and spring (Figure 2d). The highest DO levels were recorded during spring in the East Sea, while the lowest occurred in autumn in the South Sea. DO levels did not significantly differ among geographical regions, but the variations were distinct based on the season.

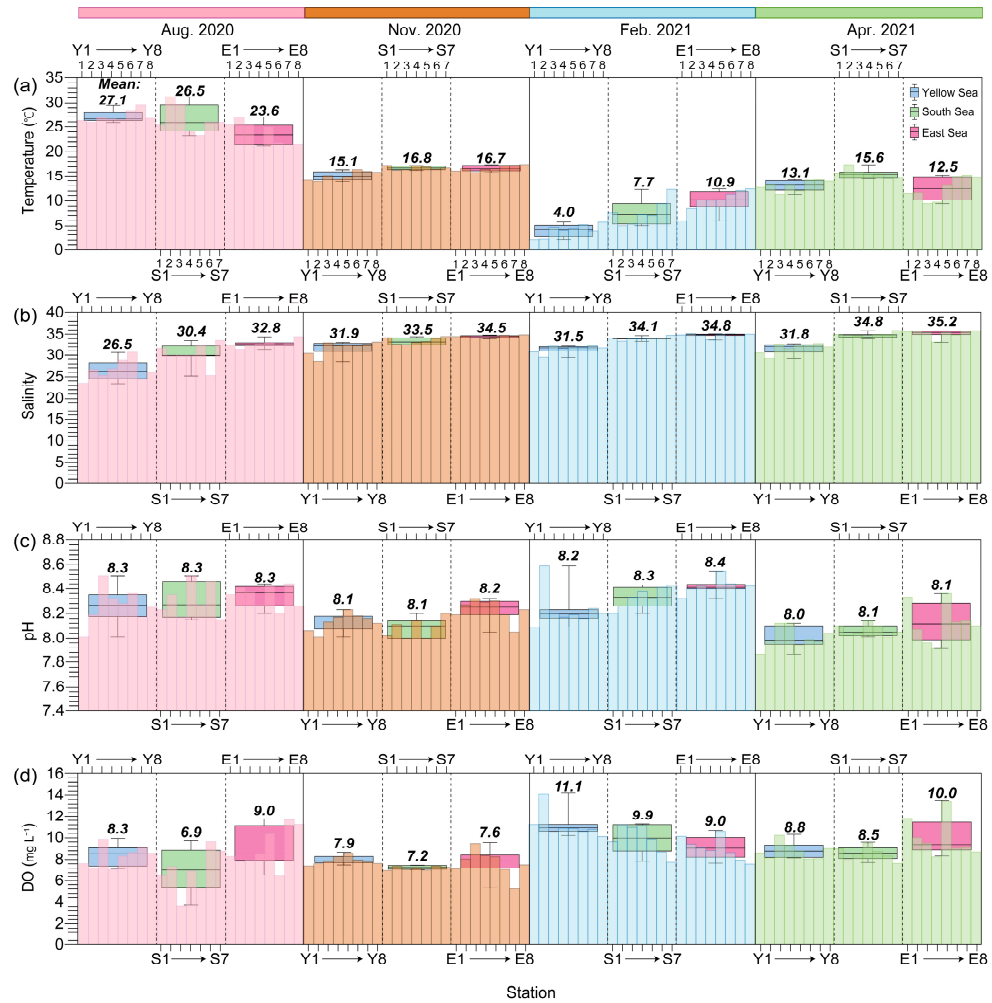


Figure 2. Values of environmental factors including temperature (a), salinity (b), pH (c), and dissolved oxygen (DO; d) at each station (bar graphs) and in three Korean coastal waters (boxplots). The letters represent the mean, and the color of the histogram indicates the season (red = summer, brown = autumn, blue = winter, green = spring).

Figure 3 illustrates the seasonal variations in dissolved inorganic nutrient concentrations at different locations, which exhibited large differences among stations. Silicate concentrations ranged from 0.80 μM at St. S3 in winter to 144 μM at St. Y6 in summer (Figure 3a). The average silicate concentrations were $29 \pm 31 \mu\text{M}$ in summer, $11 \pm 6.7 \mu\text{M}$ in autumn, $10 \pm 6.0 \mu\text{M}$ in winter, and $11 \pm 8.1 \mu\text{M}$ in spring. Nitrate + nitrite concentration was high in the East Sea in summer and remained at low levels in the spring in the South Sea. Seasonally, the average nitrite + nitrate concentrations were $17.0 \pm 19.0 \mu\text{M}$ in summer, $7.8 \pm 7.1 \mu\text{M}$ in autumn, $10.4 \pm 6.1 \mu\text{M}$ in winter, and $8.3 \pm 8.5 \mu\text{M}$ in spring (Figure 3b). Ammonia concentrations varied from 0.33 μM at St. Y5 in autumn to 66.3 μM at St. E7 in summer. The ammonia concentrations during autumn and winter were notably higher in the Yellow Sea and South Sea compared to those in the East Sea (Figure 3c) and maintained low levels in spring. The mean ammonia concentrations were $3.8 \pm 4.6 \mu\text{M}$ in summer, 4.8

$\pm 3.9 \mu\text{M}$ in autumn, $6.4 \pm 5.5 \mu\text{M}$ in winter, and $3.6 \pm 3.0 \mu\text{M}$ in spring. Overall, phosphate levels were detected at low levels (Figure 3d). The mean phosphate concentrations were $0.5 \pm 0.3 \mu\text{M}$ in winter, $0.4 \pm 0.2 \mu\text{M}$ in spring, $0.6 \pm 0.8 \mu\text{M}$ in summer, and $0.4 \pm 0.2 \mu\text{M}$ in autumn, ranging from $0.03 \mu\text{M}$ at St. Y1 in summer to $3.71 \mu\text{M}$ at St. E7 in summer. There were no significant seasonal profile differences among the three geographical regions during all four seasons ($p > 0.05$).

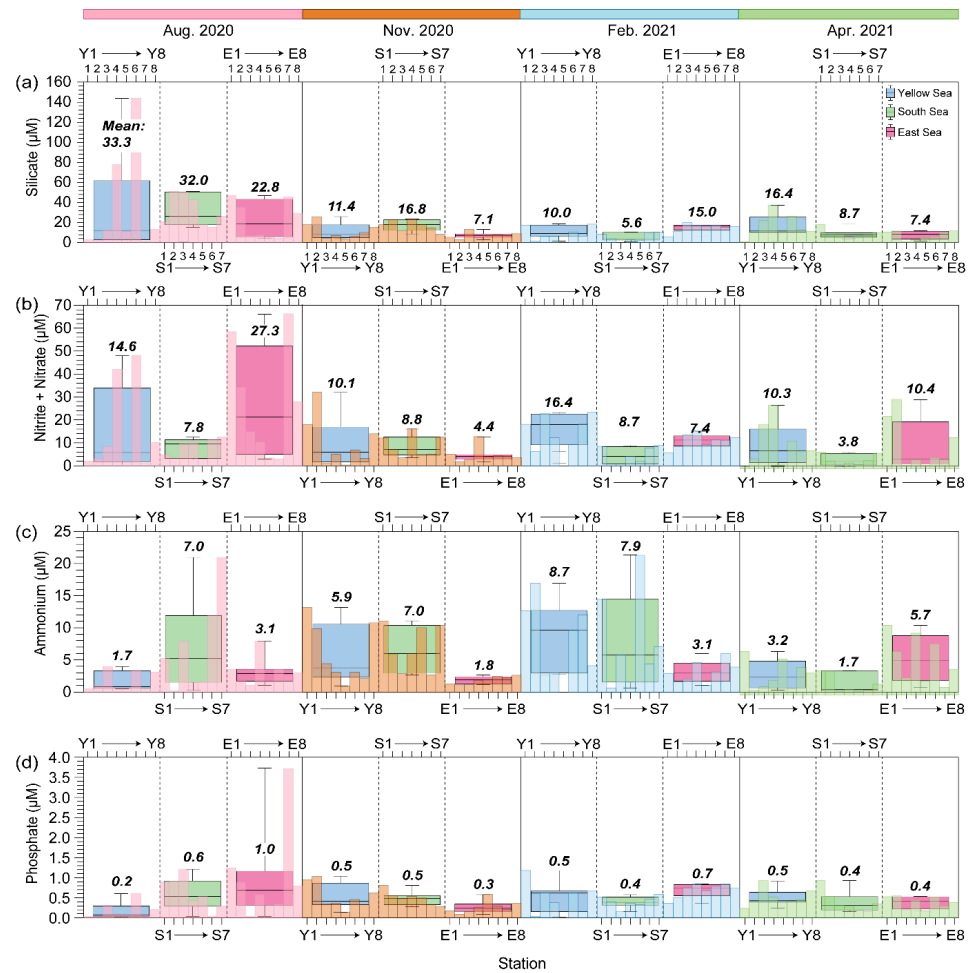


Figure 3. Concentrations of nutrients including silicate (a), nitrite + nitrate (b), ammonium (c), and phosphate (d) at each station (bar graphs) and in three Korean coastal waters (boxplots). The letters represent the mean, and the color of the histogram indicates the season (red = summer, brown = autumn, blue = winter, green = spring).

3.2. Biological Factors and Phytoplankton Community in Each Coastal Region

Table 1 shows the seasonal and spatial variations in Chl. *a* concentrations and phytoplankton abundance at each station and the differences among geographical regions. Overall, in summer, Chl. *a* was relatively higher than in other seasons (Kruskal–Wallis test; $p < 0.05$), with a mean concentration of $2.38 \pm 1.69 \mu\text{g L}^{-1}$. On the other hand, Chl. *a* was relatively low in autumn, with a mean concentration of $0.51 \pm 0.65 \mu\text{g L}^{-1}$. The highest value of Chl. *a* was observed to be $6.05 \mu\text{g L}^{-1}$ at St. Y1 in summer, while the lowest value was observed to be $0.06 \mu\text{g L}^{-1}$ at St. S4 in winter. In particular, a relatively low value of Chl. *a* in East Sea was recorded in winter season, which was observed to be $<0.3 \mu\text{g L}^{-1}$. Even in the winter season, the mean Chl. *a* concentrations in the Yellow Sea ($0.85 \pm 0.34 \mu\text{g L}^{-1}$) and South Sea ($0.76 \pm 0.32 \mu\text{g L}^{-1}$) remained at a similar level compared to that in the East Sea (Kruskal–Wallis test; $p < 0.05$). Similar to Chl. *a* concentrations, total phytoplankton abundance was high in the summer (Kruskal–Wallis test; $p < 0.05$), which was

observed to be 59.7×10^5 cells L⁻¹ at St. S7. Seasonal average total phytoplankton abundances were high in summer ($9.9 \pm 14.6 \times 10^5$ cells L⁻¹), followed by spring ($2.4 \pm 3.3 \times 10^5$ cells L⁻¹), winter ($0.7 \pm 1.2 \times 10^5$ cells L⁻¹), and autumn ($0.6 \pm 1.4 \times 10^5$ cells L⁻¹). The highest value of total phytoplankton was observed to be 59.7×10^5 cells L⁻¹ at St. S7 in summer. On the other hand, the lowest total phytoplankton was observed to be 927 cells L⁻¹ at St. Y7 in autumn. In the winter season, mean phytoplankton abundance levels in the Yellow Sea ($1.50 \pm 1.41 \times 10^5$ cells L⁻¹) and East Sea ($1.31 \pm 1.58 \times 10^5$ cells L⁻¹) were similar, but that in the South Sea ($4.61 \pm 5.47 \times 10^5$ cells L⁻¹) was higher than in the other two coastal regions.

Table 1. Seasonal changes in chlorophyll *a* and total phytoplankton abundance at each sampling station.

Coastal Region	Station Number	August 2020		November 2020		February 2021		April 2021	
		* Chl. <i>a</i>	* P.A.	Chl. <i>a</i>	P.A.	Chl. <i>a</i>	P.A.	Chl. <i>a</i>	P.A.
Yellow Sea	Y1	6.05	11.26	0.22	0.05	0.49	0.27	0.99	1.42
	Y2	3.86	4.02	0.36	0.19	3.69	5.58	0.56	1.09
	Y3	2.33	12.90	0.23	0.07	0.44	0.35	1.02	0.78
	Y4	0.54	0.86	0.29	0.28	1.08	0.33	1.58	0.86
	Y5	1.80	0.61	0.64	0.31	2.01	0.75	0.71	0.09
	Y6	1.01	0.48	0.84	0.38	0.93	0.22	0.66	0.77
	Y7	2.20	1.58	0.46	0.01	0.26	0.24	0.53	4.57
	Y8	2.62	1.09	0.38	0.05	0.36	0.11	0.74	2.46
South Sea	S1	0.69	0.13	0.27	0.13	0.20	0.05	0.75	0.31
	S2	5.14	0.87	0.40	0.11	0.84	0.79	0.61	1.21
	S3	5.73	24.76	0.82	1.15	1.54	2.51	1.21	4.12
	S4	3.59	1.82	0.41	0.14	0.06	2.13	1.09	13.12
	S5	1.88	4.55	0.30	0.11	0.66	0.59	0.85	11.65
	S6	2.44	13.61	0.48	0.23	0.12	0.23	0.48	1.28
	S7	3.83	59.70	0.30	1.13	0.08	0.10	0.33	0.61
East Sea	E1	1.55	10.41	0.11	0.10	0.29	0.12	1.57	3.58
	E2	0.37	1.98	0.24	0.41	0.13	0.35	1.40	4.11
	E3	0.43	4.61	3.37	7.17	0.06	0.57	0.12	0.78
	E4	1.87	1.75	0.48	0.53	0.07	0.21	0.19	0.56
	E5	2.22	10.22	0.16	0.27	0.06	0.17	0.30	0.48
	E6	0.12	0.27	0.37	0.28	0.14	0.09	0.32	0.23
	E7	1.34	40.41	0.22	0.20	0.12	0.23	0.24	0.52
	E8	3.24	19.34	0.36	0.57	0.18	0.07	0.06	0.21

* Chl. *a* = Chlorophyll *a* (μg L⁻¹). * P.A. = Phytoplankton abundance (×10⁵ cells L⁻¹).

Figure 4 shows the seasonal variations in phytoplankton abundances of each group at each station. Overall, Bacillariophyceae (=diatoms) exhibited high cell density in summer, reaching $8.2 \pm 14.1 \times 10^5$ cells L⁻¹, particularly at St. S7 in South Sea. Similarly, the Dinophyceae density was observed to be $1.57 \pm 3.8 \times 10^5$ cells L⁻¹ on average in summer in the South Sea. Also, the dinoflagellates peaked at 10.3×10^5 cells L⁻¹ at St. S3 in the South Sea. *Cryptomonas* spp. peaked in spring, with a highest density of $0.64 \pm 0.75 \times 10^5$ cells L⁻¹, recorded at St. E7 in the East Sea (3.5×10^5 cells L⁻¹). Three major groups contributed to the annual phytoplankton community. Of these, Bacillariophyceae significantly dominated at 60%, followed by Cryptophyceae (ave. 29%) and Dinophyceae (ave. 11%). Seasonally, diatoms were found in the highest proportion in summer, at 80%, followed by 60% in winter, 49% in spring, and 50% in autumn. The seasonal composition of Cryptophyceae was high in spring, followed by in winter, autumn, and summer. Dinophyceae

were observed at 54% in autumn but remained at <5% in the other seasons. Dinophyceae had an extremely low proportion in winter in the Yellow Sea, whereas they were recorded at a high of 77% in autumn in the East Sea (total: 7.2×10^5 cells L^{-1}) (Figure 4).

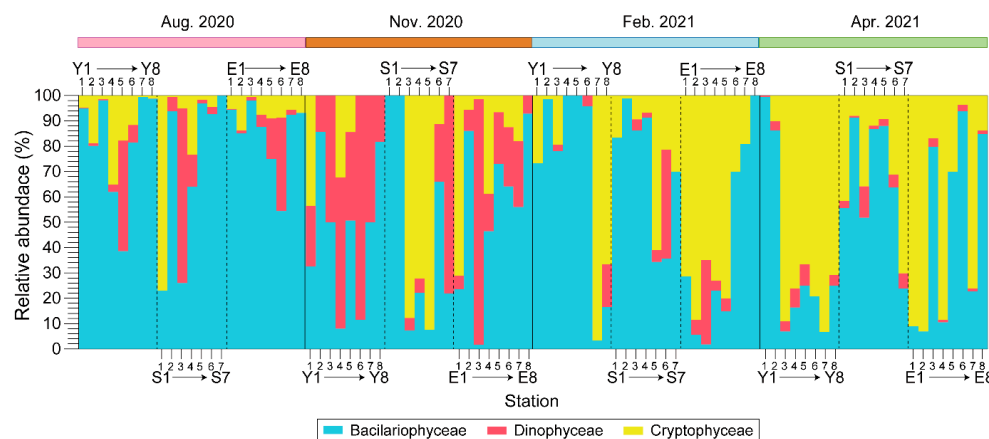


Figure 4. Composition of the major phytoplankton groups including Bacillariophyceae, Dinophyceae, and Cryptophyceae at each station in the three Korean coastal waters. The color of the histogram indicates the major phytoplankton groups (bar graph; blue = Bacillariophyceae, red = Dinophyceae, yellow = Cryptophyceae).

In the Yellow Sea, diatoms such as *Thalassiosira rotula*, *Skeletonema* spp., *Paralia sulcata*, *Eucampia zodiacus*, and *Cerataulina pelagica* prevailed in different seasons, while the dinoflagellates *Gonyaulax polygramma* and *Gyrodinium spirale* peaked in autumn at several stations (Figure 5). In summer, although the dominant diatoms varied geographically, *Skeletonema* spp. was prevalent between Stns. Y1–Y3. Additionally, *E. zodiacus* and *C. pelagica* were relatively abundant at Stns. Y4–Y5 and Y6–Y8, respectively. In autumn, there was an increase in dinoflagellates such as *G. polygramma* (Y4 = 34%, Y5 = 17%, Y6 = 63%) and *G. spirale* (Y7 = 50%), while some stations were dominated by *Cryptomonas* spp. and *P. sulcata*. During winter, *T. rotula* dominated at Station Y2, while *P. sulcata* was observed at most stations. In particular, *Cryptomonas* spp. exhibited region-specific dominance at Stns. Y7 and Y8, which are located in the lower latitudes of the Yellow Sea. In spring, *Cryptomonas* spp. was the dominant species overall, with notable peaks of *Rhizosolenia rotula*, *Guinardia striata*, and *Dactyliosolen fragilissimus*.

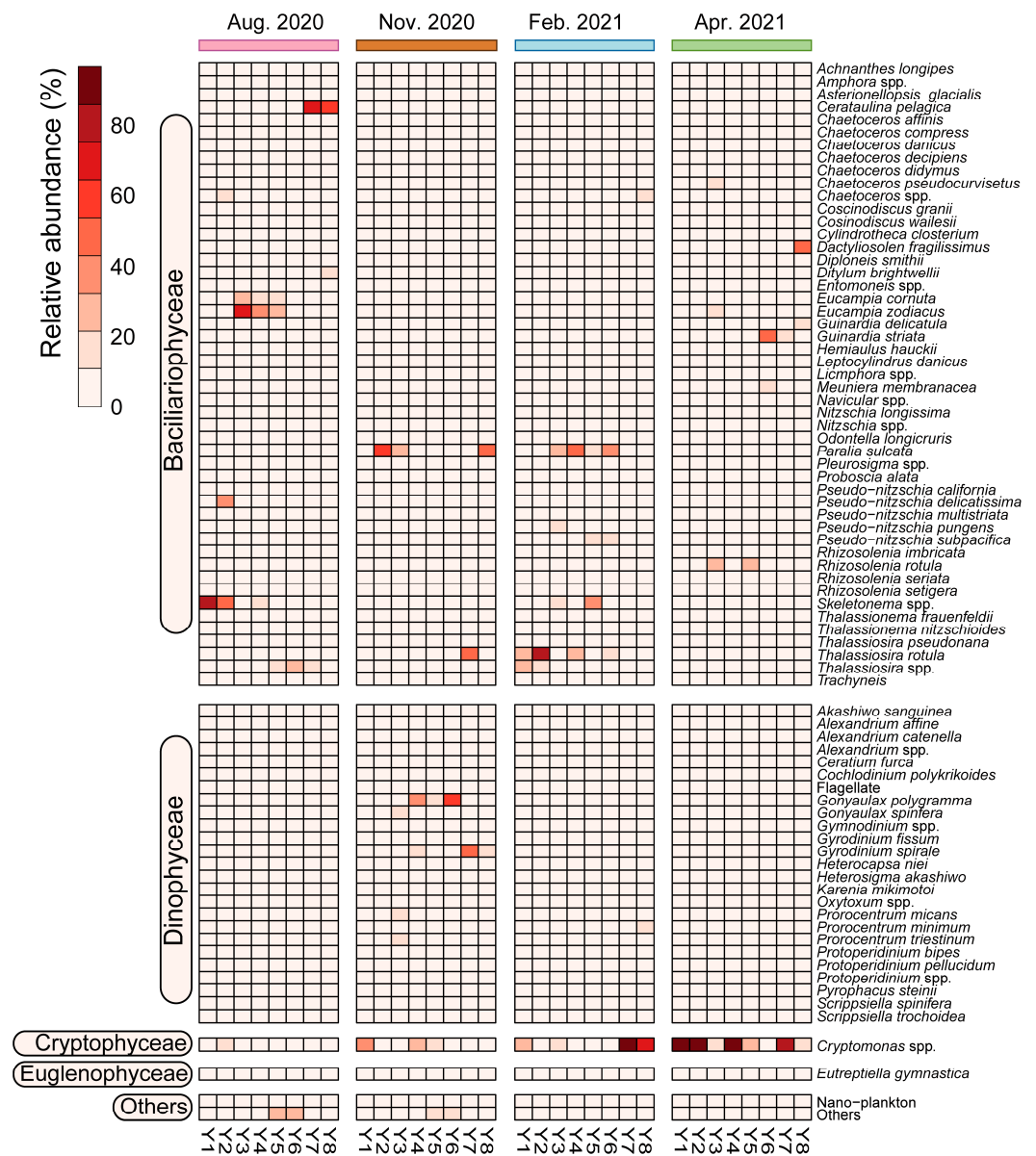


Figure 5. Changes in phytoplankton composition over seasons at each station in the Yellow Sea. Dominant species cut-off at 50% or more of the highest dominance rate at the station.

In the South Sea, *Cryptomonas* spp. (mean: 25%) and pennate diatoms of the *Pseudo-nitzschia* spp., including *P. delicatissima*, *P. subpacific*, and *P. californica*, consistently dominated. Also, seasonally, diatoms such as *Chaetoceros pseudocurvisetus*, *Talassiosira pseudonana*, and *Leptocylindrus danicus* appeared as dominant species. (Figure 6). In summer, *Cryptomonas* spp. dominated, comprising 71% at St. S1. Additionally, the distribution of the *Pseudo-nitzschia* genus expanded, and *T. pseudonana* dominated at Stns. S6 and S7. During autumn, notable dominance of *Cryptomonas* spp. occurred at Stns. S3, S4, and S5. Meanwhile, *P. sulcata* and *P. subpacific* prevailed in the western area of the region, and *Coscinodiscus granii* and *Pyrophacus steinii* dominated in the eastern area. During winter, various diatoms such as *Nitzschia* sp., *P. subpacific*, *C. pseudocurvisetus*, and *E. zodiacus* were prevalent. Additionally, *Cryptomonas* spp. was relatively abundant between Stns. S5 and S7. In spring, *L. danicus* was abundant at Stns. S5–S7, while *Cryptomonas* spp. was relatively prevalent at most stations.

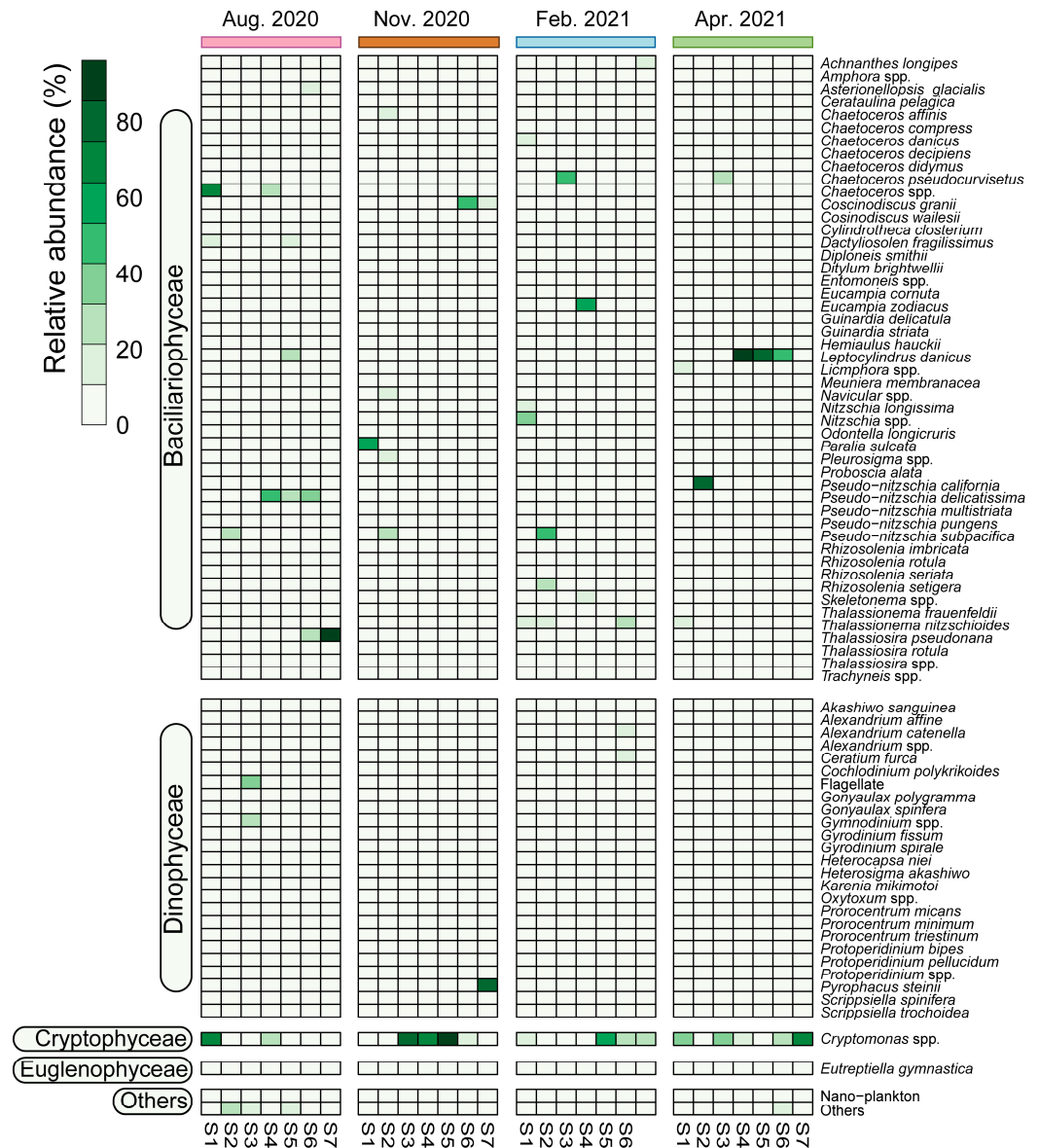


Figure 6. Changes in phytoplankton composition over seasons at each station in the South Sea. Dominant species cut-off at 50% or more of the highest dominance rate at the station.

In the East Sea, the dominant species was *Cryptomonas* spp., peaking in winter and spring (Figure 7). In the East Sea, seasonal dominant diatom species were clearly distinguished, with *Thalassiosira rotula*, *Coscinodiscus granii*, *Paralia sulcata*, and *Chaetoceros* spp. dominating in different seasons. During summer, *Cryptomonas* spp. declined sharply, with *T. pseudonana* becoming relatively abundant at most stations, except for Stns. E3–E5. Notably, at St. E5, the Euglenophyceae *Eutreptiella gymnastica* appeared and dominated with 86% abundance. In autumn, *C. granii* dominated overall, followed by *Cryptomonas* spp. and the dinoflagellate *Akashiwo sanguinea*. In winter, *Cryptomonas* spp. prevailed between Stations E1 and E5, while *P. sulcata* was dominant between Stations E3 and E8. In spring, an increase in *Chaetoceros* spp. was observed at Stns. E1 and E2, whereas high abundances of *Cryptomonas* spp. were recorded between Stns. E3 and E8.

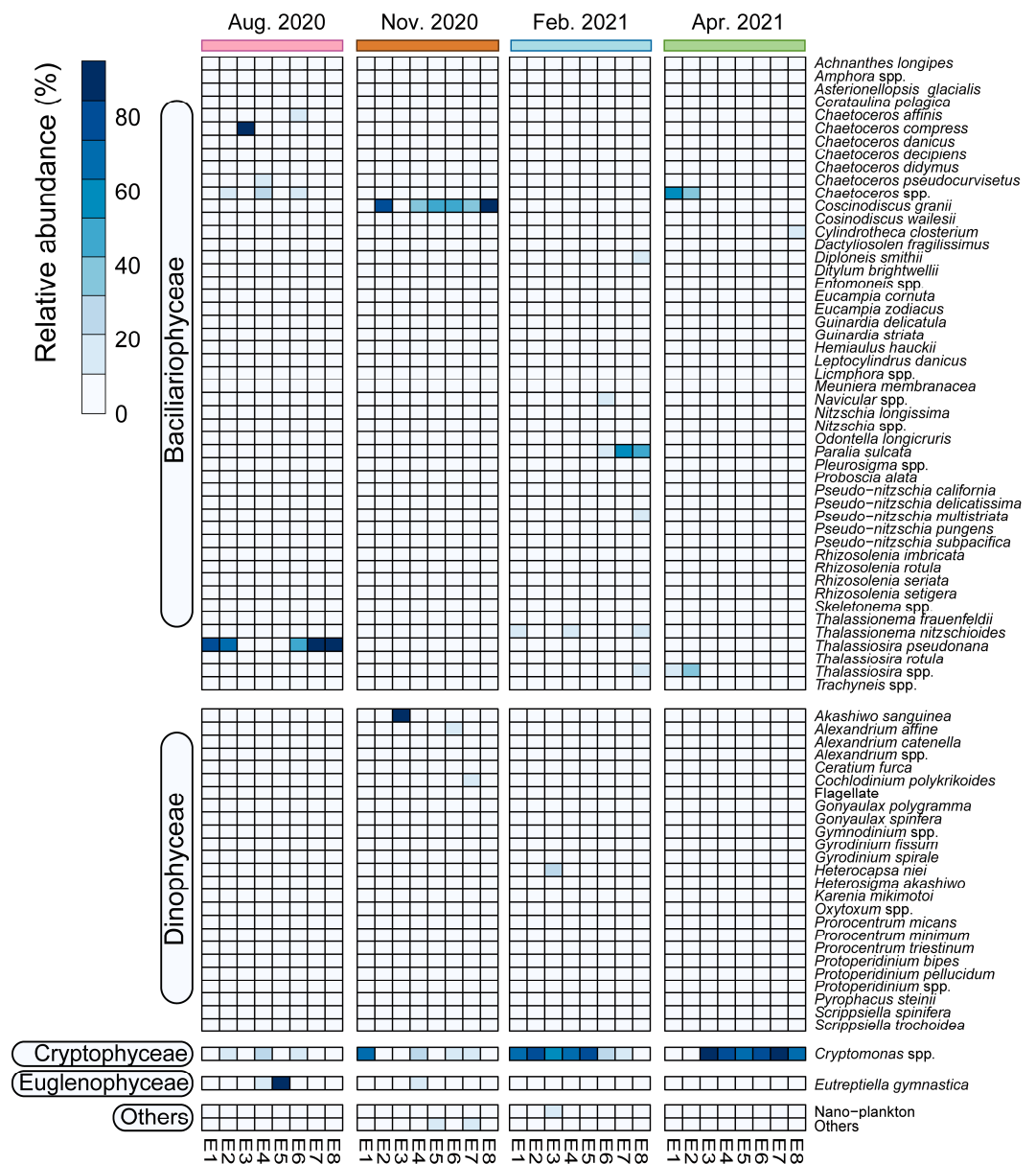


Figure 7. Changes in phytoplankton composition over seasons at each station in the East Sea. Dominant species cut-off at 50% or more of the highest dominance rate at the station.

3.3. Seasonality of Abiotic and Biotic Factors in Korean Coastal Waters

Our satellite model data indicate that during winter and spring, water temperatures are higher in the eastern area compared to the western area due to the Tsushima warm current (TWC) (Figure 8a). Particularly in summer, low-salinity water from the Changjiang River in East China Sea was introduced into the South Sea (Figure 8b). In addition, there was a clear temperature difference between the upper and lower regions of the East Sea, and it was observed that Chl. *a* concentrations were continuously maintained at a certain level (Figure 8c).

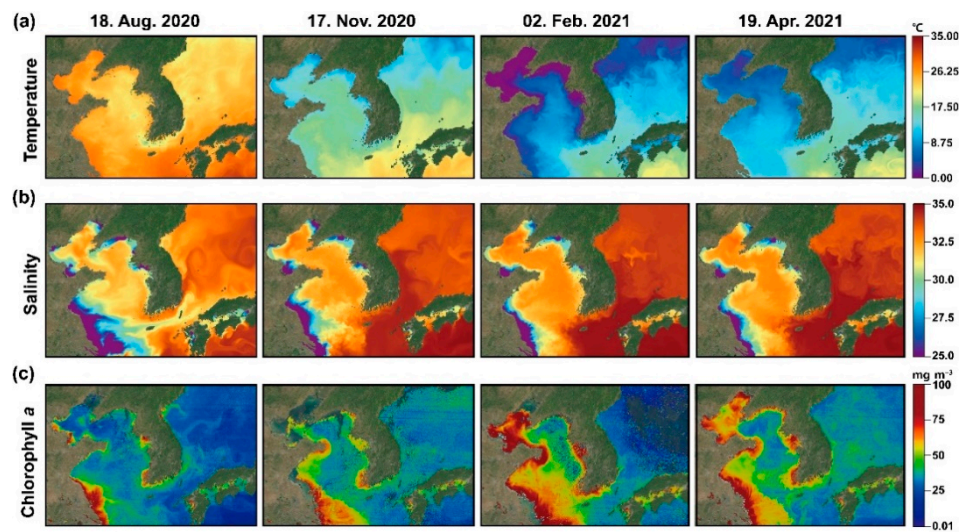


Figure 8. Satellite data provided by Japan Aerospace Exploration Agency (JAXA) at the time of the field survey. The data include sea surface temperature (a), salinity (b), and chlorophyll *a* (c).

The seasonal variations of abiotic factors, including temperature, salinity, pH, DO, and nutrients, and biotic factors commonly exhibited high variability during the summer season. Specifically, temperatures reached their annual maximum during summer and minimum during winter (Kruskal–Wallis test; $p < 0.05$) (Figure 9a). In contrast, salinity was lowest during the summer rainy season ($p < 0.05$) (Figure 9b). The pH was higher in summer and winter but lower in autumn and spring ($p < 0.05$) (Figure 9c). The DO concentrations peaked in winter ($p < 0.05$) (Figure 9d). Meanwhile, although the mean nutrient concentrations were higher in summer, with substantial spatial fluctuations, there were no significant differences ($p > 0.05$) (Figure 9e–h). On the other hand, both cell density and Chl. *a* levels were significantly higher during summer ($p < 0.05$) (Figure 9i,j).

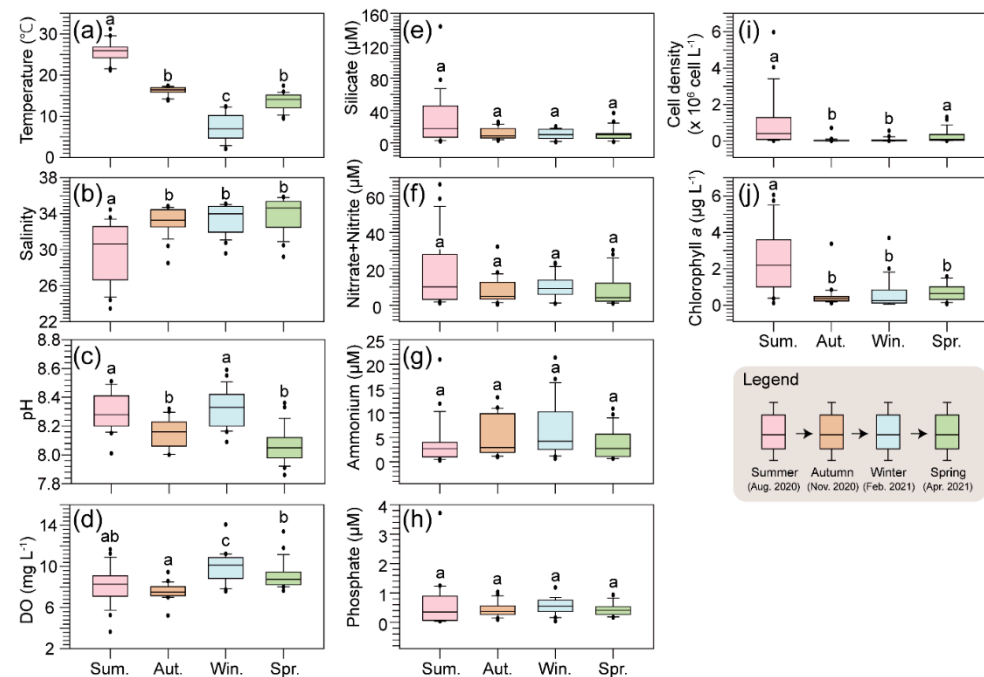


Figure 9. Box plots of seasonal variations in environmental factors including temperature (a), salinity (b), pH (c), dissolved oxygen (d); nutrients including silicate (e), nitrite+nitrate (f), ammonium (g), phosphate (h); and biological factors including cell density (i) and chlorophyll *a* (j). Letters indicate significant differences between the four seasons ($p < 0.05$; Mann–Whitney post hoc test).

Our PCA analysis showed that in the Yellow Sea (Figure 10a), the eigenvalues of Axis 1 and Axis 2 were 4.58 and 2.60, respectively. Axis 1 was influenced by water temperature, nutrients (nitrate+nitrite, phosphate, silicate) and *Skeletonema* spp., while *Cryptomonas* spp., *E. zodiacus* and water temperature played an important factor in the ordination of Axis 2. In the South Sea (Figure 10b), the eigenvalues of Axis 1 and Axis 2 were 4.35 and 2.37, respectively. Water temperature, Chl. *a*, nitrate+nitrite, silicate and *L. danicus* were the most important variables for Axis 1, whereas Axis 2 was influenced by phosphate, ammonium, and *Chaetoceros* spp. The East Sea (Figure 10c) exhibited eigenvalues of 4.27 and 2.32 for Axis 1 and Axis 2, respectively. Water temperature, salinity, Chl. *a*, *T. pseudonana*, and *Cryptomonas* spp. significantly shaped Axis 1, while nitrate+nitrite and *C. granii* were the major contributors to Axis 2. In the entire regions (Figure 10d), the eigenvalues of Axis 1 and Axis 2 were 2.76 and 2.13, respectively. Axis 1 was predominantly influenced by temperature, salinity, Chl. *a*, and silicate with Bacillariophyceae and Dinophyceae, while Axis 2 was primarily determined by nitrite+nitrate and phosphate with Bacillariophyceae.

▲ Aug. 2020 ◆ Nov. 2020 ● Feb. 2021 ■ Apr. 2021 → Phytoplankton → Environmental factors

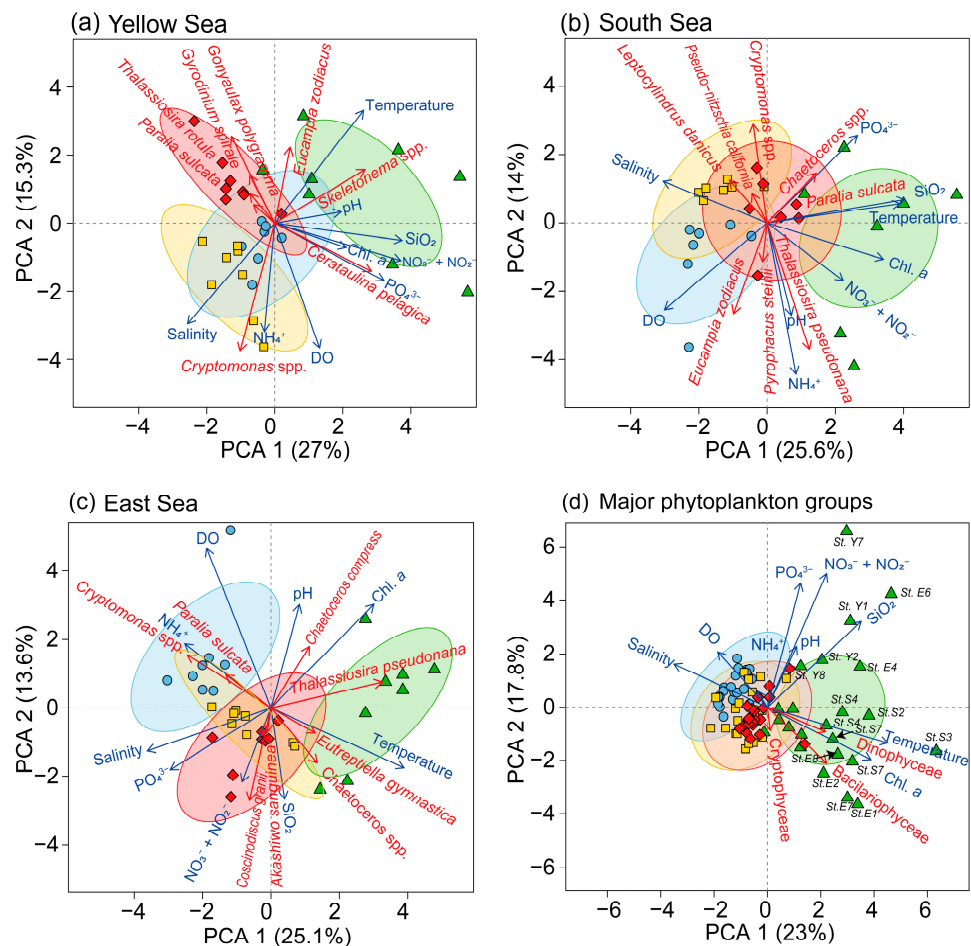


Figure 10. PCA analysis between dominant species and environmental factors in the Yellow Sea (a), South Sea (b), East Sea (c), and major phytoplankton groups (d). Ellipses indicates the 95% confidence interval for each season.

According to the seasonal relative abundance of major phytoplankton groups such as Bacillariophyceae, Cryptophyceae, and Dinophyceae (Figure 11), diatom dominance increased to 80–100% during the summer, winter, and spring seasons. On the other hand, cryptophyte dominance declined sharply from 62% to 2% when diatoms were dominant.

In particular, dinoflagellate dominance slightly increased from 30% to 80% during the autumn period, whereas diatom dominance decreased from 20% to 70% during the same period.

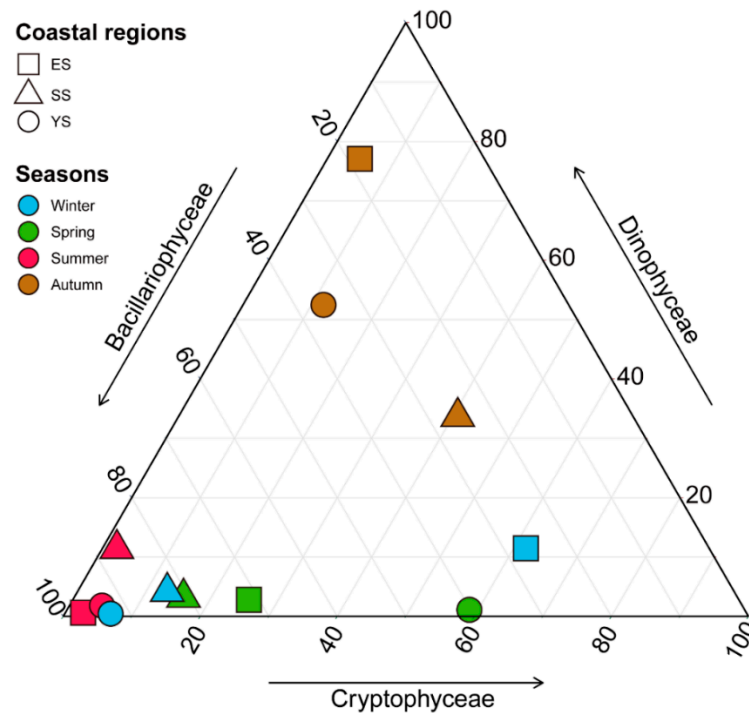


Figure 11. Seasonal relative abundance of the major phytoplankton groups including Bacillariophyceae, Dinophyceae, and Cryptophyceae in the three Korean coastal waters. The shapes of the symbols represent the coastal regions (ES = square, SS = triangle, YS = circle), and the colors of the symbols represent the seasons (winter = blue, spring = green, summer = red, autumn = brown).

4. Discussion

It is well known that the winter dry season in temperate areas is characterized by strong winds and low water temperatures, while the summer rainy season features weak winds and high water temperatures [24,28]. During spring and autumn, moderate water temperatures promote phytoplankton growth, resulting in blooms during both seasons. In the present study, there was a typical temperate seasonality pattern. Winter water temperatures in the East Sea were notably higher than in the Yellow Sea due to the influence of the Jeju warm current (JWC) and the Tsushima warm current (TWC), both branches of the Kuroshio Current [18]. In contrast, summer water temperatures in the East Sea were notably lower compared to the other two regions, highlighting the importance of deeper oceanic waters and currents in determining region-specific seasonal water temperatures. On the other hand, throughout all seasons, based on field and satellite model data, the Yellow Sea exhibited a noticeable freshwater influence from major Chinese rivers such as the Changjiang and Yellow Rivers, as well as from South Korean rivers such as the Han, Geum, and Yeongsan, resulting in low salinity levels. Conversely, the East Sea maintained higher salinity due to the influence of the TWC, particularly during all seasons except summer. Mitchell et al. [19] also demonstrated the existence of a subpolar front between latitudes 36 and 40 degrees, influenced by the East Korean warm current (EKWC) and the North Korean cold current (NKCC). These seasonal environmental characteristics significantly impact on phytoplankton population dynamics, as described below.

It is widely acknowledged that nutrient and water temperature significantly impact phytoplankton growth and seasonal species succession in coastal waters [22,24,29,30]. Moreover, light conditions, coastal currents, and grazing patterns can potentially be factors influencing the seasonal dynamics of phytoplankton [31–33]. Nutrients are primarily

introduced into these coastal waters through water mixing, upwelling events, and river runoff [22,28,34]. In particular, river discharge can typically cause high nutrient levels [28], especially during rainy seasons in temperate regions. Although a decrease in river discharge during the winter dry season often results in reduced nutrient input to coastal water [35], water mixing can compensate the euphotic layer by providing sufficient nutrients. However, in this study, nutrient levels have remained relatively consistent during the winter season, suggesting that phytoplankton might not have utilized them effectively, particularly in the East Sea (winter mean Chl. *a*: 0.13 $\mu\text{g L}^{-1}$). As a consequence, the elevated introduction of nutrients into coastal waters during periods of high water temperatures stimulated the proliferation of phytoplankton, resulting in an increased Chl. *a* concentration.

Generally, during the summer season, if additional nutrient supply does not follow the peak bloom of spring phytoplankton in the upper layer of the euphotic zone, a consistently low nutrient level is observed, leading to sustained low productivity of phytoplankton. Interestingly, this study observed consistently high levels of Chl. *a* and phytoplankton abundance in summer. Specifically, average Chl. *a* concentration and total phytoplankton abundances in the field were notably high in coastal regions, especially in the East Sea. This characteristic was also evident in satellite data, confirming the presence of high Chl. *a* levels aligned with the flow of ocean currents. Such satellite images closely matched the Chl. *a* data observed during field surveys. Consequently, the maintenance of high Chl. *a* across the Korean Peninsula during the summer season is likely heavily influenced by nutrient supply from rainfall, showing different characteristics from other years or seasons. According to our satellite image data, the elevated Chl. *a* was transported into offshore waters by ocean currents, indicating that the coastal phytoplankton blooms contributed to the primary production of the open ocean, particularly in summer in the East Sea.

In the Yellow Sea, diatoms predominantly occupied the waters in summer, autumn, and spring, while dinoflagellates were more prevalent in autumn. During summer, *Skeletonema* spp. and *Eucampia zodiacus* were the most abundant. *E. zodiacus* is distributed globally and sometimes forms dense blooms in Tokyo Bay [36], Harimanada [37], and the Ariake Sea [38]. *E. zodiacus* has been observed under high nutrient conditions during winter and spring at the Seomjin River mouth and Gwangyang Bay [28]. *Skeletonema* spp. blooms often occur in nutrient-rich conditions in summer in Dokai Bay, one of the most eutrophic embayments in Japan, as demonstrated by Kaeriyama et al. [39] and Yamada et al. [40]. In PCA analysis, two diatoms, *Skeletonema* spp. and *E. zodiacus*, showed a positive correlation with water temperature, implying they have an advantage over other algal species in high water temperatures, even with high nutrient levels. In addition, according to PCA, *G. polygramma* and *G. spirale* have a negative correlation with Chl. *a* and nutrients such as nitrite+nitrate and phosphate, implying that both dinoflagellates have an advantage in the absence of diatom proliferation. On the other hand, *T. rotula* (53%) and *P. sulcata* (31%) were well maintained under the high nutrient conditions of winter. *T. rotula* is known to grow particularly well in low-temperature environments during winter in temperate regions, as demonstrated by Sin et al. [41], Mönnich et al. [42], and our previous study [25]. In spring, *Cryptomonas* spp. (52%) were mainly observed together with *Rhizosolenia rotula*, *Guinardia striata*, and *Dactyliosolen fragilissimus* at several sites, implying that large-sized diatoms can grow in low water temperatures and exhibit region-specific responses. As a result, the Yellow Sea, characterized by low salinity, high nutrient levels, strong tidal mixing, and river discharge, was favorable for diatom growth in nutrient-rich and turbulent environments. In contrast, dinoflagellates and *Cryptomonas* spp. had an advantage in the absence of diatom proliferation.

In the South Sea, groups of phytoplankton were distinguished seasonally. Notably, a significant diatom bloom was observed in the summer and spring, with an increase in *Chaetoceros* spp. during the summer and *Pseudo-nitzschia* spp. during the spring. Additionally, *Leptocylindrus danicus* was abundant in the central area of the South Sea in spring.

The genus *Chaetoceros speies* is well known as a cosmopolitan species that sometimes forms dense blooms in coastal waters [43], significantly contributing to phytoplankton communities worldwide [44]. Moreover, Baek et al. [24] reported that *Leptocylindrus danicus*, *Chaetoceros* spp., and *Pseudo-nitzschia* spp. accounted for approximately 85% of the total phytoplankton in the Nakdong River estuary and Busan coasts during spring, showing a similar trend to our study in the South Sea. In particular, *Pseudo-nitzschia* species and *L. danicus* showed negative correlations with nitrate+nitrite, while *T. pseudonana* exhibited a positive correlation. On the other hand, *Chaetoceros* spp. had a positive correlation with phosphate, implying that taxon-specific responses were influenced by seasonal nutrient levels. As a result, the South Sea, characterized by moderate salinity, nutrient levels, tidal mixing, and river discharge compared to the Yellow Sea, showed a seasonal response to diatom growth, depending on whether the waters were nutrient-rich or nutrient-poor, influenced by region-specific characteristics.

In the East Sea, the small diatom *Thalassiosira pseudonana* maintained notably high densities during the summer, while the large diatom *Coscinodiscus granii* showed high densities at most stations during the autumn. Interestingly, *Cryptomonas* spp. exhibited high densities during both winter and spring. Additionally, the euglenophyte *Eutreptiella gymnastica* was prevalent in the summer, while the dinoflagellate *Akashiwo sanguinea* experienced significant blooms at certain stations in the autumn. Baek et al. [45] demonstrated in culture experiments that *T. pseudonana* populations grew significantly with increasing temperatures (10–30 °C) in brackish and marine waters, indicating their adaptation to euryhaline and eurythermal conditions. The negative correlation between salinity and *T. pseudonana* in our PCA analysis supports their tolerance to low-salinity conditions. *Cryptomonas* spp. showed positive correlations with ammonia but negative associations with temperature, suggesting a preference for low water temperatures. *E. gymnastica* exhibited a positive correlation with water temperature, indicating a preference for higher water temperatures. The large diatom *C. granii* was influenced by nitrite+nitrate and silicate concentrations, suggesting a requirement for major nutrients to maintain its large cell size and division. In summary, the East Sea, characterized by its open ocean environment, exhibited a clear seasonal response of phytoplankton, influenced by the prevalence of small diatoms in summer, large diatoms in autumn, and *Cryptomonas* spp. thriving in relatively cold water temperatures during winter and spring. Additionally, the ability of phytoplankton to adapt to seasonal water temperatures depended on region-specific characteristics such as ocean currents and open ocean environments.

Marshall and Lacouture [46] reported seasonal fluctuations in the biomass of *Cryptomonas* spp., with higher biomass in the summer and autumn and lower biomass in the winter. In the present study, however, *Cryptomonas* spp. tended to be relatively dominant in environments with low temperatures, such as during winter and spring, and in conditions with low Chl. *a* concentrations, which contrasts with the findings of Marshall and Lacouture [46]. On the other hand, cryptophytes acquire nutrients via a mixotrophic mode, switching from utilizing dissolved nutrients to feeding [47,48], which can give them an advantage over other diatom species under nutrient-limited conditions. Additionally, *Cryptomonas* spp. are characterized by opportunistic dominance in nutrient-limited environments with relatively few competitors [24,49,50]. In the present study, *Cryptomonas* spp. were well adapted to low water-temperature conditions and the absence of diatoms along the Korean coasts. Clay et al. [51] demonstrated that cryptophytes are a cosmopolitan phytoplankton group found under a wide range of environmental conditions. Our PCA analysis showed a positive association between Bacillariophyceae and chlorophyll *a* levels, whereas Cryptophyceae exhibited an inverse relationship, suggesting their propensity to thrive when diatom proliferation is suppressed. Based on our results and previous reports, cryptophytes may be more influenced by the presence of diatoms rather than by nutrient levels and water temperature alone. In other words, temperature affects nutrient consumption by phytoplankton, and lower-temperature seasons can slightly

delay the proliferation of phytoplankton. In the absence of diatom proliferation, *Cryptomonas* spp. may exhibit opportunistic dominance in the coastal microalga ecosystem.

It is important to understand how the dominant group within a phytoplankton niche changes with variations in environmental conditions because it reveals the underlying mechanisms of phytoplankton bloom dynamics associated with group-specific or species-specific ecological and physiological features. Our results showed distinct seasonal shifts in the three major phytoplankton groups in Korean coastal waters: diatoms sharply increased in the three geographical regions during summer (80–100%), and dinoflagellates remained high in autumn, particularly in the East Sea. Cryptophyceae moderately increased in the Yellow Sea in spring, the East Sea in winter, and the South Sea in autumn, depending on region- and season-specific characteristics. Our results imply that Cryptophyceae moderately increased in abundance when diatoms were not dominant, occurring in spring in the Yellow Sea, winter in the East Sea, and autumn in the South Sea. This implies that cryptophytes play an important role as opportunistic species in Korean coastal waters, as described above. Consequently, the seasonal succession from diatoms to cryptophytes or dinoflagellates has been confirmed, and this understanding is crucial for determining the succession of phytoplankton group levels.

Our findings demonstrate distinct differences in phytoplankton community and biomass based on seasonal physicochemical features in three coastal waters of Korea. The Yellow Sea, characterized by low salinity, high nutrient levels, strong tidal mixing, and river discharge, favored diatom growth in nutrient-rich and turbulent conditions. The South Sea, with its moderate salinity, nutrient levels, and tidal mixing, exhibited seasonal variations in diatom growth depending on nutrient availability, influenced by local environmental characteristics. The East Sea, an open ocean environment, displayed distinct seasonal phytoplankton patterns: small diatoms in summer, large diatoms in autumn, and *Cryptomonas* spp. in the colder waters of winter and spring. This region-specific information on phytoplankton, the basis of the marine food web, is expected to serve as foundational data for various marine industries, including the selection of optimal sites for aquaculture of commercial macroalgae and fish.

5. Summaries and Conclusions

Our key findings highlight the complex interactions between seasonal water temperature, salinity, nutrient, and phytoplankton community structure in the coastal waters of the Yellow Sea, South Sea, and East Sea of Korea. The distinct environmental characteristics such as ocean currents, freshwater input, and tidal mixing in each region highlight the unique ecological dynamics of each marine environment. Ocean currents were a major factor leading to a warm winter in the East Sea, as well as seasonal temperature differences. The nutrient-rich environment facilitated significant phytoplankton growth. Additionally, the high summer chlorophyll *a* concentrations observed in satellite data indicate the influence of coastal blooms on marine primary production. In particular, Bacillariophyceae emerged as significant contributors to phytoplankton biomass in all regions, despite seasonal environmental changes. Interestingly, despite the dominance of these diatoms, seasonal fluctuations in phytoplankton groups such as Cryptophyceae and Dinophyceae suggest that their ability to adapt to different environmental conditions may allow them to opportunistically exploit ecological niches. Our findings, which shed light on the regional and seasonal variability in phytoplankton dynamics, suggest that microecosystem monitoring is necessary in various coastal waters of the Korean Peninsula for effective management and conservation of coastal ecosystems, and are of important value as fundamental data.

Author Contributions: Conceptualization, S.H.B.; Validation, Y.K.L. and S.H.B.; Formal analysis, C.H.L., Y.K.L. and M.K.; Investigation, Y.K.L., M.K. and S.H.B.; Data curation, C.H.L.; Writing – original draft, C.H.L. and S.H.B.; Writing—review & editing, Y.K.L., S.H. and S.H.B.; Visualization,

C.H.L.; Supervision, S.H.B.; Funding acquisition, S.H. All authors have read and agreed to the published version of the manuscript.

Funding: This research was supported by grant (20163MFDS641) from the Ministry of Food and Drug Safety, Republic of Korea. This research was also supported by a project on the sustainable research and development of Dokdo (PG54141), which is funded by the Ministry of Oceans and Fisheries, Republic of Korea.

Institutional Review Board Statement: Not applicable.

Informed Consent Statement: Not applicable.

Data Availability Statement: The raw data supporting the conclusions of this article will be made available by the authors, without undue reservation, to any qualified researcher.

Acknowledgments: Research product of temperature, salinity, chlorophyll *a* (produced from Himawari-8) that was used in this paper was supplied by the P-Tree System, Japan Aerospace Exploration Agency (JAXA), Chōfu, Japan.

Conflicts of Interest: The authors declare that they have no known competing financial interests or personal relationships that could have appeared to influence the work reported in this paper.

References

1. Cloern, J.E.; Foster, S.Q.; Kleckner, A.E. Phytoplankton primary production in the world's estuarine-coastal ecosystems. *Biogeosciences* **2014**, *11*, 2477–2501.
2. Naselli-Flores, L.; Padišák, J. Ecosystem services provided by marine and freshwater phytoplankton. *Hydrobiologia* **2023**, *850*, 2691–2706.
3. Basu, S.; Mackey, K.R. Phytoplankton as key mediators of the biological carbon pump: Their responses to a changing climate. *Sustainability* **2018**, *10*, 869.
4. Ramesh, R.; Chen, Z.; Cummins, V.; Day, J.; D'elia, C.; Dennison, B.; Forbes, D.; Glaeser, B.; Glaser, M.; Glavovic, B. Land–ocean interactions in the coastal zone: Past, present & future. *Anthropocene* **2015**, *12*, 85–98.
5. Neumann, B.; Vafeidis, A.T.; Zimmermann, J.; Nicholls, R.J. Future coastal population growth and exposure to sea-level rise and coastal flooding—a global assessment. *PLoS ONE* **2015**, *10*, e0118571.
6. Cloern, J.E. Our evolving conceptual model of the coastal eutrophication problem. *Mar. Ecol. -Prog. Ser.* **2001**, *210*, 223–253.
7. Thompson, P.A.; Bonham, P.I.; Swadling, K.M. Phytoplankton blooms in the Huon Estuary, Tasmania: Top-down or bottom-up control? *J. Plankton Res.* **2008**, *30*, 735–753.
8. Guinder, V.A.; Popovich, C.A.; Molinero, J.C.; Marcovecchio, J. Phytoplankton summer bloom dynamics in the Bahía Blanca Estuary in relation to changing environmental conditions. *Cont. Shelf Res.* **2013**, *52*, 150–158.
9. Baek, S.H.; Son, M.; Kim, D.; Choi, H.W.; Kim, Y.O. Assessing the ecosystem health status of Korea Gwangyang and Jinhae bays based on a planktonic index of biotic integrity (P-IBI). *Ocean Sci. J.* **2014**, *49*, 291–311.
10. Gobler, C.J.; Berry, D.L.; Dyhrman, S.T.; Wilhelm, S.W.; Salamov, A.; Lobanov, A.V.; Zhang, Y.; Collier, J.L.; Wurch, L.L.; Kustka, A.B. Niche of harmful alga *Aureococcus anophagefferens* revealed through ecogenomics. *Proc. Natl. Acad. Sci. USA* **2011**, *108*, 4352–4357.
11. Alexander, H.; Rouco, M.; Haley, S.T.; Wilson, S.T.; Karl, D.M.; Dyhrman, S.T. Functional group-specific traits drive phytoplankton dynamics in the oligotrophic ocean. *Proc. Natl. Acad. Sci. USA* **2015**, *112*, E5972–E5979.
12. Litchman, E.; Edwards, K.F.; Klausmeier, C.A.; Thomas, M.K. Phytoplankton niches, traits and eco-evolutionary responses to global environmental change. *Mar. Ecol. -Prog. Ser.* **2012**, *470*, 235–248.
13. Brun, P.; Vogt, M.; Payne, M.R.; Gruber, N.; O'Brien, C.J.; Buitenhuis, E.T.; Le Quéré, C.; Leblanc, K.; Luo, Y.W. Ecological niches of open ocean phytoplankton taxa. *Limnol. Oceanogr.* **2015**, *60*, 1020–1038.
14. Alexander, H.; Jenkins, B.D.; Rynearson, T.A.; Dyhrman, S.T. Metatranscriptome analyses indicate resource partitioning between diatoms in the field. *Proc. Natl. Acad. Sci. USA* **2015**, *112*, E2182–E2190.
15. Lie, H.J.; Cho, C.H. Seasonal circulation patterns of the Yellow and East China Seas derived from satellite-tracked drifter trajectories and hydrographic observations. *Prog. Oceanogr.* **2016**, *146*, 121–141.
16. Chang, Y.; Chan, J.W.; Huang, Y.C.A.; Lin, W.Q.; Lee, M.A.; Lee, K.T.; Liao, C.H.; Wang, K.Y.; Kuo, Y.C. Typhoon-enhanced upwelling and its influence on fishing activities in the southern East China Sea. *Int. J. Remote Sens.* **2014**, *35*, 6561–6572.
17. Jin, X.; Tang, Q. Changes in fish species diversity and dominant species composition in the Yellow Sea. *Fish Res.* **1996**, *26*, 337–352.
18. Isoda, Y.; Saitoh, S.I. The northward intruding eddy along the east coast of Korea. *J. Oceanogr.* **1993**, *49*, 443–458.
19. Mitchell, D.; Watts, D.; Wimbush, M.; Teague, W.; Tracey, K.; Book, J.; Chang, K.I.; Suk, M.S.; Yoon, J.H. Upper circulation patterns in the Ulleung Basin. *Deep-Sea Res. Part II Top. Stud. Oceanogr.* **2005**, *52*, 1617–1638.
20. Lee, J.Y.; Kang, D.J.; Kim, I.N.; Rho, T.; Lee, T.; Kang, C.K.; Kim, K.R. Spatial and temporal variability in the pelagic ecosystem of the East Sea (Sea of Japan): A review. *J. Mar. Syst.* **2009**, *78*, 288–300.

21. Chang, K.I.; Teague, W.; Lyu, S.; Perkins, H.; Lee, D.K.; Watts, D.; Kim, Y.B.; Mitchell, D.; Lee, C.; Kim, K. Circulation and currents in the southwestern East/Japan Sea: Overview and review. *Prog. Oceanogr.* **2004**, *61*, 105–156.
22. Baek, S.H.; Lee, M.; Park, B.S.; Lim, Y.K. Variation in phytoplankton community due to an autumn typhoon and winter water turbulence in southern Korean coastal waters. *Sustainability* **2020**, *12*, 2781.
23. Lee, M.; Park, B.S.; Baek, S.H. Tidal influences on biotic and abiotic factors in the Seomjin River Estuary and Gwangyang Bay, Korea. *Estuaries Coasts* **2018**, *41*, 1977–1993.
24. Baek, S.H.; Kim, D.; Kim, Y.O.; Son, M.; Kim, Y.-J.; Lee, M.; Park, B.S. Seasonal changes in abiotic environmental conditions in the Busan coastal region (South Korea) due to the Nakdong River in 2013 and effect of these changes on phytoplankton communities. *Cont. Shelf Res.* **2019**, *175*, 116–126.
25. Lim, Y.K.; Hong, S.; Lee, C.H.; Kim, M.G.; Baek, S.H. Influence of region-specific marine environments on phytoplankton and bacterial communities in the Korean coastal waters during winter. *Ocean Sci. J.* **2024**, in submitted.
26. Sournia, A. *Phytoplankton Manual*; United Nations Educational, Scientific and Cultural Organization: Paris, France, 1978; ISBN 92-3-101572-9.
27. Omura, T.; Iwataki, M.; Borja, V.M.; Takayama, H.; Fukuyo, Y. *Marine Phytoplankton of the Western Pacific*; Kouseisha Kouseikaku: Tokyo, Japan, 2012; p. 160.
28. Baek, S.H.; Kim, D.; Son, M.; Yun, S.M.; Kim, Y.O. Seasonal distribution of phytoplankton assemblages and nutrient-enriched bioassays as indicators of nutrient limitation of phytoplankton growth in Gwangyang Bay, Korea. *Estuar. Coast. Shelf Sci.* **2015**, *163*, 265–278.
29. Wang, G.; Cao, W.; Yang, Y.; Zhou, W.; Liu, S.; Yang, D. Variations in light absorption properties during a phytoplankton bloom in the Pearl River estuary. *Cont. Shelf Res.* **2010**, *30*, 1085–1094.
30. Yoon, J.N.; Lee, M.; Jin, H.; Lim, Y.K.; Ro, H.; Park, Y.G.; Baek, S.H. Summer distributional characteristics of surface phytoplankton related with multiple environmental variables in the Korean coastal waters. *J. Mar. Sci. Eng.* **2022**, *10*, 850.
31. Marzetz, V.; Spijkerman, E.; Striebel, M.; Wacker, A. Phytoplankton community responses to interactions between light intensity, light variations, and phosphorus supply. *Front. Environ. sci.* **2020**, *8*, 539733.
32. Chen, Y.; Sun, X.; Zhun, M. Net-phytoplankton communities in the Western Boundary Currents and their environmental correlations. *J. Oceanol. Limnol.* **2018**, *36*, 305–316.
33. Tan, Y.; Huang, L.; Chen, Q.; Huang, X. Seasonal variation in zooplankton composition and grazing impact on phytoplankton standing stock in the Pearl River Estuary, China. *Cont. Shelf Res.* **2004**, *24*, 1949–1968.
34. Jin, H.; Zhang, C.; Meng, S.; Wang, Q.; Ding, X.; Meng, L.; Zhuang, Y.; Yao, X.; Gao, Y.; Shi, F. Mock, T.; Gao, H. Atmospheric deposition and river runoff stimulate the utilization of dissolved organic phosphorus in coastal seas. *Nat. Commun.* **2024**, *15*, 658.
35. Kim, J.H.; Lee, M.; Lim, Y.K.; Kim, Y.J.; Baek, S.H. Occurrence characteristics of harmful and non-harmful algal species related to coastal environments in the southern sea of Korea. *Mar. Freshw. Res.* **2019**, *70*, 794–806.
36. Yoshida, K.; Chiba, S.; Ishimaru, T. Long-term variation in the wintertime diatom community structure in Tokyo Bay, Japan (1981–2000). *Plankton Benthos Res.* **2011**, *6*, 195–205.
37. Nishikawa, T.; Hori, Y.; Tanida, K.; Imai, I. Population dynamics of the harmful diatom *Eucampia zodiacus* Ehrenberg causing bleachings of *Porphyra thalli* in aquaculture in Harima-Nada, the Seto Inland Sea, Japan. *Harmful Algae* **2007**, *6*, 763–773.
38. Ito, Y.; Katano, T.; Fujii, N.; Koriyama, M.; Yoshino, K.; Hayami, Y. Decreases in turbidity during neap tides initiate late winter blooms of *Eucampia zodiacus* in a macrotidal embayment. *J. Oceanogr.* **2013**, *69*, 467–479.
39. Kaeriyama, H.; Katsuki, E.; Otsubo, M.; Yamada, M.; Ichimi, K.; Tada, K.; Harrison, P.J. Effects of temperature and irradiance on growth of strains belonging to seven *Skeletonema* species isolated from Dokai Bay, southern Japan. *Eur. J. Phycol.* **2011**, *46*, 113–124.
40. Yamada, M.; Katsuki, E.; Otsubo, M.; Kawaguchi, M.; Ichimi, K.; Kaeriyama, H.; Tada, K.; Harrison, P.J. Species diversity of the genus *Skeletonema* (Bacillariophyceae) in the industrial harbor Dokai Bay, Japan. *J. Oceanogr.* **2010**, *66*, 755–771.
41. Sin, Y.; Lee, E.; Lee, Y.; Shin, K.H. The river–estuarine continuum of nutrients and phytoplankton communities in an estuary physically divided by a sea dike. *Estuar. Coast. Shelf Sci.* **2015**, *163*, 279–289.
42. Mönnich, J.; Tebben, J.; Bergemann, J.; Case, R.; Wohlrab, S.; Harder, T. Niche-based assembly of bacterial consortia on the diatom *Thalassiosira rotula* is stable and reproducible. *ISME J.* **2020**, *14*, 1614–1625.
43. Malviya, S.; Scalco, E.; Audic, S.; Vincent, F.; Veluchamy, A.; Poulain, J.; Wincker, P.; Iudicone, D.; De Vargas, C.; Bittner, L. Insights into global diatom distribution and diversity in the world’s ocean. *Proc. Natl. Acad. Sci. USA* **2016**, *113*, E1516–E1525.
44. Suzuki, Y.; Takahashi, M. Growth responses of several diatom species isolated from various environments to temperature. *J. Phycol.* **1995**, *31*, 880–888.
45. Baek, S.H.; Jung, S.W.; Shin, K. Effects of temperature and salinity on growth of *Thalassiosira pseudonana* (Bacillariophyceae) isolated from ballast water. *J. Freshw. Ecol.* **2011**, *26*, 547–552.
46. Marshall, H.G.; Lacouture, R. Seasonal patterns of growth and composition of phytoplankton in the lower Chesapeake Bay and vicinity. *Estuar. Coast. Shelf Sci.* **1986**, *23*, 115–130.
47. Tranvik, L.J.; Porter, K.G.; Sieburth, J.M. Occurrence of bacterivory in *Cryptomonas*, a common freshwater phytoplankton. *Oecologia* **1989**, *78*, 473–476.
48. Rottberger, J.; Gruber, A.; Boenigk, J.; Kroth, P.G. Influence of nutrients and light on autotrophic, mixotrophic and heterotrophic freshwater chrysophytes. *Aquat. Microb. Ecol.* **2013**, *71*, 179–191.

49. Klaveness, D. Biology and ecology of the Cryptophyceae: Status and challenges. *Biol. Oceanogr.* **1989**, *6*, 257–270.
50. Pålsson, C.; Granéli, W. Nutrient limitation of autotrophic and mixotrophic phytoplankton in a temperate and tropical humic lake gradient. *J. Plankton Res.* **2004**, *26*, 1005–1014.
51. Clay, B.L.; Kugrens, P.; Lee, R.E. A revised classification of Cryptophyta. *Bot. J. Linnean Soc.* **1999**, *131*, 131–151.

Disclaimer/Publisher's Note: The statements, opinions and data contained in all publications are solely those of the individual author(s) and contributor(s) and not of MDPI and/or the editor(s). MDPI and/or the editor(s) disclaim responsibility for any injury to people or property resulting from any ideas, methods, instructions or products referred to in the content.